Recombinant Osteopontin Improves Neurological Functional Recovery and Protects Against Apoptosis via PI3K/Akt/GSK-3β Pathway Following Intracerebral Hemorrhage

Authors' Contribution:
Study Design A
Data Collection B
Statistical Analysis C
Data Interpretation D
Manuscript Preparation E
Literature Search F
Funds Collection G

AE 1 Wenqian Zhang
BF 2 Ying Cui
AF 3,4 Junling Gao
CD 3,4 Ran Li
BF 3,4 Xiaohua Jiang
D 3,4 Yanxia Tian
BC 2 Kaijie Wang
AE 1,2 Jianzhong Cui

1 Department of Surgery, Hebei Medical University, Shijiazhuang, Hebei, P.R. China
2 Department of Neurosurgery, Tangshan Gongren Hospital, Tangshan, Hebei, P.R. China
3 School of Basic Medical Science, North China University of Science and Technology, Tangshan, Hebei, P.R. China
4 Hebei Key Laboratory for Chronic Diseases, Tangshan Key Laboratory for Preclinical and Basic Research on Chronic Diseases, Tangshan, Hebei, P.R. China

Corresponding Author: Jianzhong Cui, e-mail: jianzhongcuidoctor@163.com
Source of support: This study was supported by a grant from the Natural Science Foundation of Hebei, China (grant no. H2012401071 and H2014105079)

Background: This study aimed to investigate the potential neuroprotective effect of recombinant osteopontin (r-OPN) on apoptotic changes via modulating phosphoinositide-3-kinase/Akt/glycogen synthase kinase 3 beta (PI3K/Akt/GSK-3β) signaling in a rat model of intracerebral hemorrhage (ICH).

Material/Methods: We subjected 10–12-week-old Sprague-Dawley male rats (n=120) to injection of autologous blood into the right basal ganglia to induce ICH or sham surgery. ICH animals received vehicle administration, r-OPN (4 μL/pup), or r-OPN combined with phosphatidylinositol 3-kinase (PI3K) inhibitor wortmannin (86 ng/pup) at 30 min after injury. Neurological scores and rotarod latencies were evaluated on days 1–5 post-ICH. Brain water content was evaluated on days 1–3 post-ICH. The number of apoptotic cells changes were evaluated by terminal deoxynucleotidyl transferase-mediated 2-deoxyuridine 5-triphosphate-biotin nick-end labeling (TUNEL) and hematoxylin staining. Apoptosis-related proteins Bcl-2, Bax, and cleaved caspase-3 (CC3), and the phosphorylation levels of Akt and GSK-3β were assayed by Western blot.

Results: Neurological deficits, rotarod latencies, and brain water content following ICH were reduced in the r-OPN group compared to the vehicle group. r-OPN also attenuated cell death in ICH. Furthermore, treatment with r-OPN significantly increased p-Akt expression and decreased p-GSK-3β. These effects were associated with a decrease in the Bax/Bcl-2 ratio and the suppression of CC3 at 24 h after ICH. Importantly, all the beneficial effects of r-OPN in ICH were abrogated by the PI3K inhibitor wortmannin.

Conclusions: r-OPN may provide a wide range of neuroprotection by suppressing apoptosis through the PI3K/Akt/GSK-3β signaling pathway after ICH.

MeSH Keywords: Apoptosis • Cerebral Hemorrhage • Osteopontin • Phosphatidylinositol 3-Kinases

Full-text PDF: https://www.medscimonit.com/abstract/index/idArt/905700

📄 3313   ▦ —   📊 5   📖 46
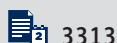
Background

Intracerebral hemorrhage (ICH) accounted for 9% to 27% of all strokes worldwide in the last decade, with poor functional outcome and high early case fatality [1–3]. Despite this devastating personal and societal impact, ICH remains an understudied disease with little improvement in patient outcomes over the last 20 years [4]. Studies have demonstrated that ICH-induced neurological damage can be divided into primary and secondary brain injury. Primary injury evoked by the physical destruction due to rapid hematoma formation in the brain parenchyma leads to brain tissue compression or disruption, as well as elevated intracranial pressure. Subsequent development of various parallel pathological processes such as neuroinflammation, neuronal apoptosis, and excitotoxicity contribute to secondary injury [5,6]. Apoptosis is a prominent form of cell death associated with ICH in the perihematomal region [7,8]. ICH has long been reported to cause neuronal apoptosis leading to declines in neurological functions [9]. Considering intact neurons as the basis of normal neurological functions, inhibition of neuronal apoptosis and alleviating neurological deficits are helpful to the patient's long-term prognosis.

Osteopontin (OPN) is a secreted extracellular matrix (ECM) glycoprotein that is involved in both physiological and pathological processes in a wide range of tissues [10]. There is compelling evidence that endogenous OPN is the most highly upregulated factor after central nervous system disease [11,12]. It can regulate inflammation, tissue remodeling, and cell survival in the field of stroke injury [10,13,14]. For example, recombinant osteopontin (r-OPN) reduced cortical neuron death via the activation the phosphatidylinositol 3-kinase (PI3K) -Akt signaling pathway kinase and increased expression of pro-survival genes in ischemic stroke [13]. Moreover, r-OPN provided neuroprotection by anti-apoptotic action in subarachnoid hemorrhage and exerted an anti-inflammatory effect by downregulating inducible NO synthase (iNOS) in ICH [14,15]. Nevertheless, until now, no published study investigated the effect of r-OPN administration on the apoptotic changes associated with recovery of neurological function during ICH.

Glycogen synthase kinase 3β (GSK-3β) is a serine/threonine kinase known to be important in cell proliferation and apoptosis signaling pathways [16,17]. The stimulated GSK-3β has been found to exacerbate brain injury in experimental ischemic stroke, traumatic brain injury, and ICH [18–20]. The pro-apoptotic role of GSK-3β has previously been shown to be negatively regulated through the phosphoinositol-3-kinase (PI3-kinase)-Akt survival pathway [21,22]. Further studies of r-OPN and interconnected anti-apoptotic mechanisms will help to develop new therapeutic targets to reduce cell death and to explore neuroprotective properties after ICH. In this study, we investigated the role of r-OPN in amelioration of brain edema and to improve neurological outcomes and behavioral outcomes by inhibiting apoptosis in a rat model of ICH. The PI3K/Akt/GSK-3β pathway was hypothesized and tested as the possible mechanism of r-OPN effects.

Material and Methods

Animals and ICH Model

Adult male Sprague-Dawley rats (11–13 weeks, 280–320 g) were used in the study. The procedures for this study were approved by the Animal Care and Use Committee of Hebei Medical University and were carried out in accordance with the Guide for the Chinese Council on Animal Protection. All rats were housed under conditions of controlled temperature and humidity. Rats had free access to food and water before and after surgery or sham treatment. Our injury model was adapted from a previously described model of ICH in rats [23]. The rats were anesthetized with 0.4% pentobarbital sodium intraperitoneally. Through the tail vein, we removed 50 ml of autologous whole blood. Using stereotaxic guidance, we administered autologous whole blood into the right caudate putamen. The stereotactic coordinates were: 0.2 mm anterior, 3.0 mm lateral to bregma, and 5.5 mm ventral. The sham group only had needle insertion. After slowly withdrawing the injection needle 10 min after injection, sealed with zinc phosphate cement, the incision was closed and disinfected with local iodine. The animals were allowed to recover spontaneous ventilation. In the course of the establishment of the experimental group in the ICH model, a total of 10 rats died.

Experimental groups and treatment

We randomly assigned 150 adult rats to 5 groups (n=30): the sham group, the vehicle (ICH+vehicle) group, the r-OPN (ICH+r-OPN) group, r-OPN+Wort (ICH+r-OPN+ wortmannin) group, and the Wort (ICH+Wortmannin) group. Mouse r-OPN (0.1 μg in 1 μL of sterile PBS; EMD chemicals, La Jolla, CA) or vehicle (1 μL; sterile PBS) were intracerebroventricularly injected at 1 h after ICH. The PI3K inhibitor wortmannin (15 μg/kg; Sigma-Aldrich, St Louis, MO) was administered before the induction of ICH. In the sham, the needle was inserted, with no administration of drug.

Brain water content

Rats were anesthetized and euthanized on days 1–3 after ICH to coincide with the point of maximum apoptotic changes. The procedure was carried out as previously described [24]. Brains were sectioned in the mid-sagittal plane, and hemispheres were weighed immediately ("wet" weight). Then, the hemispheres were dried at 80°C for 24 h, and "dry" weight was measured.

We calculated water content as a percentage of wet weight ([wet weight–dry weight]/[wet weight]×100).

Neurological score

Modified neurological severity score (mNSS) is a composite of motor tests, sensory tests, beam balance tests, and reflexes absent [25]. In our study, it was used to grade various aspects of neurobehavioral function on days 1–5 after ICH. Lower scores indicate better function (normal score=0), and higher scores indicate more severe injury (maximal deficit score=18).

Rotarod test

An accelerating automated rotarod was used to measure the effects of therapeutic intervention on vestibulomotor function [26]. The speed was slowly increased from 4 to 40 rpm within 5 min. When the rats were dropped twice from the ladder of the device, the experiment ended. On 3 days before the ICH injury, the rats were pretrained, and the average time elapsed from the rotation of the cylinder was recorded as the baseline latency. To assess early motor outcome, mice underwent rotarod testing on days 1–5 after injury. Average latency to fall from the rod was recorded.

Apoptosis analysis by terminal deoxynucleotidyl transferase-mediated (dUTP) nick-end labeling (TUNEL) staining

A modified method for analysis of apoptosis in paraffin-embedded sections using TUNEL staining has been described previously [28]. Briefly, the rats that were randomly selected for anesthetization with chloral hydrate were perfused transcardially with ice-cold saline, followed by 4% paraformaldehyde in 0.1 M phosphate buffer, to pre-fix the brain tissue. Brain tissue specimen from the cerebral hemorrhage area were excised and fixed in 4% paraformaldehyde for 48 h, embedded in paraffin, and then cut into serial sections (5-μm). After deparaffinization and rehydration, the paraffin sections were rinsed in 0.1 M phosphate-buffered saline (PBS) twice and incubated with Proteinase K working solution (10 μg/ml in 10 mM Tris/HCl, pH 7.5–8.0) for 15 min at 37°C. After being washed in PBS again, the sections were treated with green fluorescein-labeled dUTP solution that contains 10% TdT. Finally, the paraffin sections were counterstained with DAPI. In apoptotic cells, TUNEL-positive cells that exhibit green fluorescent granules were determined using a microscope and were quantified by randomly selecting 5 microscopic fields to count.

Western blot analysis

Western blot analysis was carried out as described previously [25]. Briefly, after administration of an overdose of chloral hydrate, rats were sacrificed at different time points after surgery. Brain tissue, except for the caudate putamen tissues surrounding the hematoma, was instantly frozen at −80°C until use. To detect protein expression, an appropriate amount of frozen brain tissue samples was minced with eye scissors in ice. Then, the tissue was homogenized in cold lysis buffer and then clarified by centrifuging (12000×g for 20 min at 4°C) before taking the supernatant. Protein concentration was determined using the Bradford method. The samples were subjected to SDS-polyacrylamide gel electrophoresis to resolve and were transferred onto a polyvinylidene fluoride (PVDF) filter membrane by a transfer apparatus at 350 mA for 2 h. Following blocked with 5% fat-free dry milk, the membrane was then incubated overnight with primary antibody at 4°C, including Actin (anti-goat, 1: 2000, Santa Cruz Biotechnology), p-GSK-3β (anti-rabbit, 1: 1000, Abcam), GSK-3β (anti-rabbit, 1: 1000, Abcam), p-Akt (anti-mouse, 1: 1000, Abcam), Akt (anti-mouse, 1: 1000, Abcam), cleaved caspase-3 (CC3, anti-mouse, 1: 1000; Cell Signaling), caspase-3 (anti-mouse, 1: 1000; Cell Signaling), Bcl-2 (anti-rabbit, 1: 1000, Cell Signaling Technology), and Bax (anti-mouse, anti-1000, Cell Signaling Technology). Nitrocellulose membranes were then labeled with secondary antibodies for 1 h at room temperature.

Statistical analyses

All data are presented as the mean ±SD and were analyzed using SPSS 17.0. The data were analyzed by one-way ANOVA, followed by Tukey's post hoc analysis. Differences were considered statistically significant for values of $P<0.05$

Results

r-OPN alleviated brain edema and attenuated neurofunctional deficits

The brain water content was analyzed in the injured hemisphere on days 1–3 after ICH induction. The brain water content was significantly increased in the vehicle group compared with the sham group ($P<0.05$, Figure 1). The rats treated with r-OPN showed reduced brain edema content compared with the vehicle group ($P<0.05$, Figure 1). However, the rats receiving r-OPN combined with PI3K inhibitor wortmannin (r-OPN+Wort) did not have reduced brain edema compared to the r-OPN group ($P<0.05$, Figure 1). Wortmannin did not increase brain edema when administered alone compared with the vehicle group ($P>0.05$, Figure 1). There was no significant difference in brain water content between the vehicle group and r-OPN+Wort group ($P>0.05$, Figure 1). The mNSS scores and rotarod testing provide a comprehensive evaluation of neurological functions in rats. There was a significant increase in mNSS score of the vehicle group compared to the sham group
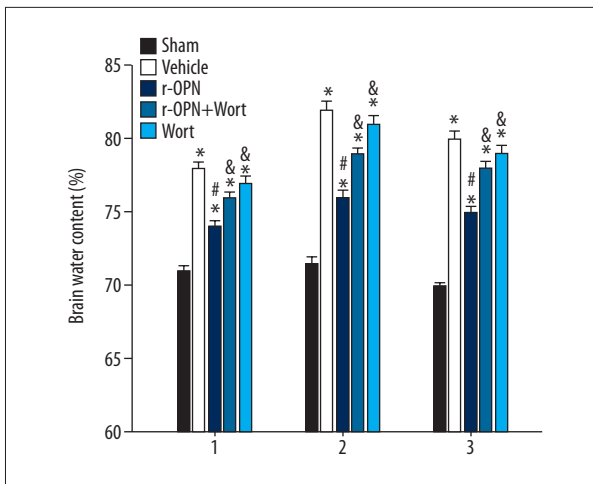
Figure 1. Brain water content was reduced in r-OPN mice at days 1–3 after ICH. Data in bar graphs are expressed as mean ±SEM. (* *P*<0.05 compared with sham, # *P*<0.05 compared with vehicle, & *P*<0.05 compared with r-OPN, n=6–8/group).

over 5 days after ICH (*P*<0.05, Figure 2A). r-OPN significantly decreased mNSS scores compared to the vehicle group (*P*<0.05, Figure 2A). When r-OPN was combined with the PI3K inhibitor wortmannin (r-OPN+Wort), mNSS scores were higher than in the r-OPN group (*P*<0.05, Figure 2A). Wortmannin did not increase mNSS when administered alone compared with the vehicle group (*P*>0.05, Figure 2A). There was no significant difference in mNSS between the vehicle group and r-OPN+Wort group (*P*>0.05, Figure 2A). ICH induced a significant decrease in rotarod latencies compared to the sham group (*P*<0.05, Figure 2B). The rotarod latencies of r-OPN-treated mice were

significantly longer than that of vehicle-treated mice (*P*<0.05, Figure 2B), whereas r-OPN+Wort group animals lagged behind the r-OPN group (*P*<0.05, Figure 2B). Wortmannin did not induce a significant decrease of rotarod latencies when administered alone compared with the vehicle group (*P*>0.05, Figure 2B). There was no significant difference in rotarod latencies between the vehicle group and r-OPN+Wort group (*P*>0.05, Figure 2B).

r-OPN administration attenuated the number of apoptotic cells at 24 h after ICH

To examine the role of r-OPN in apoptosis, TUNEL/DAPI staining revealed a high density of positively stained cells within the hemorrhagic lesion itself as well as in the surrounding periphery. TUNEL staining was localized with the nuclei marker DAPI (Figure 3A). Quantitative analysis showed regional TUNEL-positive cell differences between the groups. Few TUNEL-positive apoptotic cells were found in the sham group. In vehicle groups, the apoptotic index in the perihematomal area was found to be significantly increased compared with those in the sham group (*P*<0.05, Figure 3B). r-OPN significantly decreased TUNEL-positive cells compared with the vehicle group (*P*<0.05, Figure 3B). Administration of r-OPN combined with wortmannin treatment increased the number of apoptotic cells, which abolished the anti-apoptotic effect of r-OPN alone (*P*<0.05, Figure 3B). There was no significant difference in the number of apoptotic cells between the vehicle group and r-OPN+Wort group (*P*>0.05, Figure 3B).
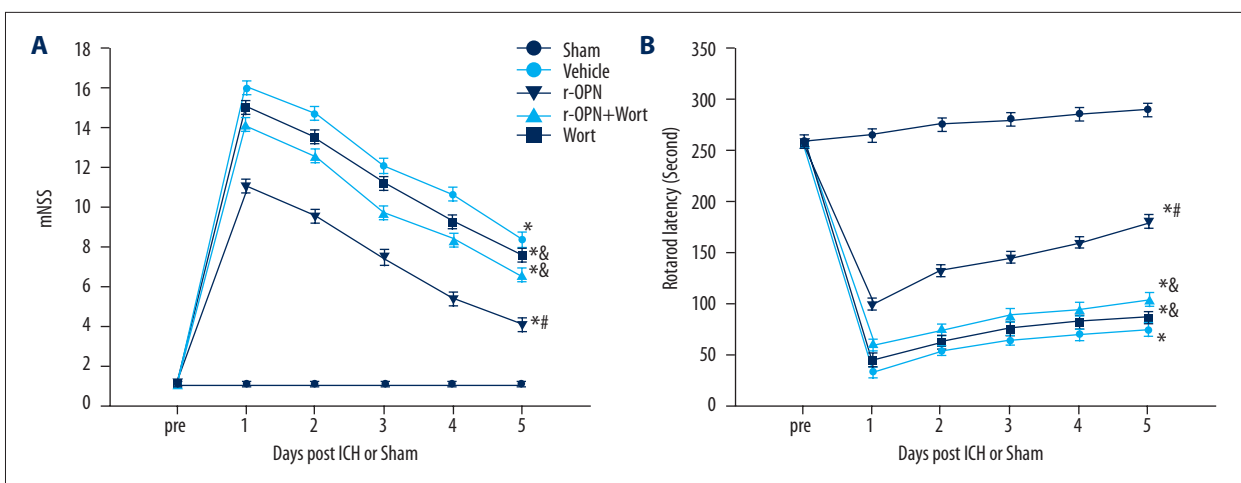

Figure 2. Neurological function showed short-term improvement in r-OPN mice over 5 days following ICH, based on neurobehavioral function and rotarod motor test. The r-OPN treatment significantly decreased the mNSS scores compared with vehicle group at 1–5 days after injury (**A**). The vestibulomotor performance by rotarod testing was also significantly improved in r-OPN group at 1–5 days after injury (**B**). Data are presented as the mean ±SEM (* *P*<0.05 compared with sham, # *P*<0.05 compared with vehicle, & *P*<0.05 compared with r-OPN, n=6–8/group).

This work is licensed under Creative Common Attribution-NonCommercial-NoDerivatives 4.0 International (CC BY-NC-ND 4.0)

1591

Indexed in: [Current Contents/Clinical Medicine] [SCI Expanded] [ISI Alerting System] [ISI Journals Master List] [Index Medicus/MEDLINE] [EMBASE/Excerpta Medica] [Chemical Abstracts/CAS]
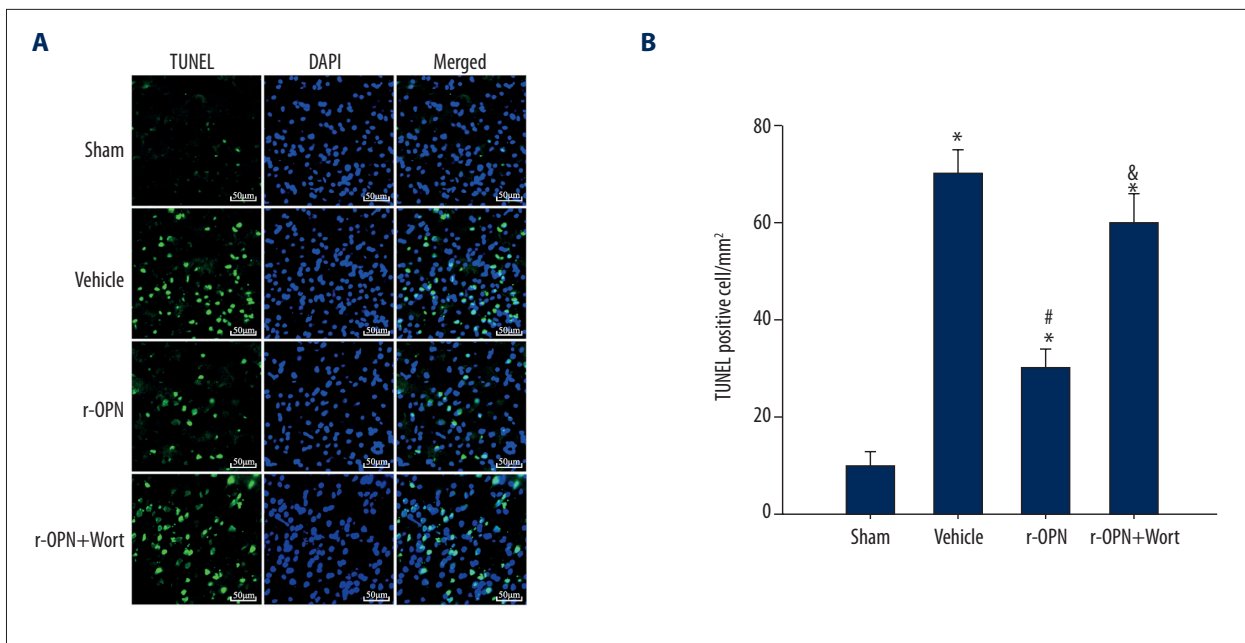
Figure 3. Co-staining of TUNEL (green) and DAPI (blue) in the perihematomal cerebral cortex at 24 h after ICH. TUNEL-positive cells were barely detected in the sham group but were widely distributed in the perihematomal area after ICH. r-OPN decreased the amounts of TUNEL-positive cells, which was blocked by wortmannin. Scale bar 50 μm (**A**). ICH increased the number of TUNEL-positive cells compared with sham group. r-OPN remarkably attenuated the number of TUNEL-positive cells, whereas wortmannin combined with r-OPN reversed the decreasing trend compared with only r-OPN treatment (**B**). Data are presented as the mean ±SEM (* P<0.05 compared with sham, # P<0.05 compared with vehicle, & P<0.05 compared with r-OPN, n=4–5/group).

r-OPN downregulated the ratio of Bax/Bcl-2 and decreased the CC3 (cleaved caspase-3) at 24 h after ICH

Bcl-2 is an anti-apoptotic factor and is important for cell survival, while Bax promotes apoptosis. A low ratio of Bax and Bcl-2 favors cell survival. Western blot analysis revealed a remarkably increased ratio of Bax/Bcl-2 in the vehicle group compared with the sham group (P<0.05, Figure 4A). r-OPN treatment significantly down-regulated the ratio of Bax/Bcl-2 compared with the vehicle group (P<0.05, Figure 4A). r-OPN restored Bax and Bcl-2 expression levels after ICH, and this protection was hindered by wortmannin (r-OPN+Wort) administration (P<0.05, Figure 4A). There was no significant difference in the ratio of Bax/Bcl-2 between the vehicle group and r-OPN+Wort group (P>0.05, Figure 4A). CC3 is an important marker of apoptosis. Western blot analysis revealed a remarkably increase of CC3 in the vehicle group compared with the sham group (P<0.05, Figure 4B). r-OPN treatment significantly decreased the level of CC3 compared with the vehicle group (P<0.05, Figure 4B), whereas treatment with wortmannin combined with r-OPN clearly increased CC-3 expression compared with r-OPN at 24 h after ICH (P<0.05, Figure 4B). There was no significant difference in CC3 between the vehicle group and the r-OPN+Wort group (P>0.05, Figure 4B). The expression of total caspase-3 was constant in the control and experimental groups (P>0.05, Figure 4B).

r-OPN activated the PI3K-Akt signaling pathway and decreased protein expressions of p-GSK-3β at 24 h after ICH

Akt is a prosurvival kinase and is activated by phosphorylation at Ser473 via the PI3K pathway, which is thought to be one of the molecules that promote cell survival and prevent apoptosis. The pro-apoptotic role of GSK-3β is an important downstream target of the Akt signaling pathway. Phosphorylation of GSK-3β on the inactivating residue serine-9 by Akt results in GSK-3β inactivation. Western blot analysis showed decreased p-Akt expression after ICH compared with sham (P<0.05, Figure 5A). r-OPN administration dramatically increased p-Akt expression compared with the vehicle group (P<0.05, Figure 5A), and this expression was reversed by PI3K inhibitor wortmannin (r-OPN+Wort) administration (P<0.05, Figure 5A). There was no statistical difference in p-Akt between the vehicle group and r-OPN+Wort group (P>0.05, Figure 5A). The expression of total Akt was constant in control and experimental groups (P>0.05, Figure 5A). Western blot analysis showed ICH dramatically increased the levels of p-GSK-3β compared with sham (P<0.05, Figure 5B). Treatment with r-OPN significantly decreased the levels of p-GSK-3β compared with the vehicle group (P<0.05, Figure 5B), whereas, treatment with r-OPN plus wortmannin obviously increased GSK-3β levels compared with r-OPN alone
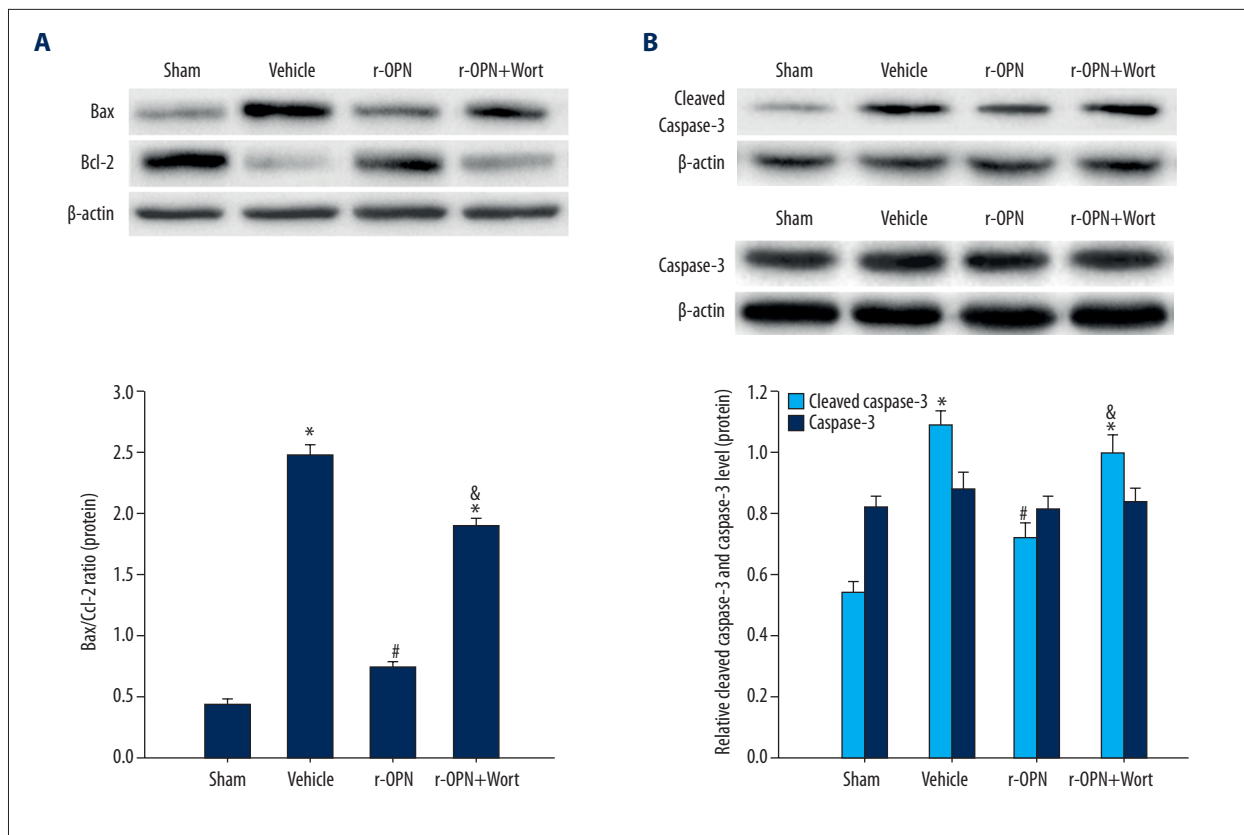
Figure 4. r-OPN affects Bcl-2 family and cleaved caspase-3 protein expression 24 h after ICH or sham. Representative Western blots and densitometric quantification of Bax/Bcl-2 (**A**). Representative Western blots and densitometric quantification and cleaved caspase-3/β-actin and total caspase-3/β-actin at 24 h after ICH (**B**). Data are presented as the mean ±SEM (* $P<0.05$ compared with sham, # $P<0.05$ compared with vehicle, & $P<0.05$ compared with r-OPN, n=6–8/group).

($P<0.05$, Figure 5B). There was no significant difference in p-GSK-3β between the vehicle group and r-OPN+Wort group ($P>0.05$, Figure 5B). The expression of total GSK-3β were constant in control and experimental groups ($P>0.05$, Figure 5B).

Discussion

In the present study, we found that r-OPN improves functional outcomes, alleviates brain edema, and reduces cell apoptosis by regulating apoptosis-related PI3K/Akt/GSK-3β signaling pathways in a preclinical rat model of ICH. ICH induced initial hematoma expansion and resultant mass effect injury, secondary to the hematoma resulting in ischemia, edema, intense inflammation, and ultimately cell death and neurological deficits [5,29]. Apoptosis is a prominent form of cell death in the perihematomal region after ICH [8]. As apoptosis is a reversible process, research has been focused on the apoptotic pathways involved in neuronal death after ICH to identify important therapeutic targets [30]. OPN is a phosphorylated glycoprotein, which is a soluble cytokine capable of stimulating signal transduction pathways in many different types of

cells [31]. There is compelling evidence that OPN can, in a variety of situations, help cells survive an otherwise lethal insult [12]. Endogenous OPN induction has consistently been found to have protective effects on ischemic injuries involving the brain and other organs [32–34]. A previous study revealed that r-OPN alleviates brain damage in a rat model of ICH by inhibiting the expression of inflammation-related iNOS, thereby suppressing matrix metalloproteinase (MMP)-9 activation [10]. Moreover, r-OPN markedly reduced the infarct size via anti-apoptotic actions in a transient focal cerebral ischemia mouse model [14]. Experimentally applied ICH induced neurological deficits and brain edema accompanied by neuronal apoptosis in rats [7]. However, the effect of r-OPN on apoptosis associated with neurological recovery in ICH remains poorly elucidated. In the current study, r-OPN alleviated apoptosis within the hemorrhagic lesion itself as well as in the surrounding periphery at 24 h after ICH. r-OPN also significantly attenuated ICH-induced brain edema on days 1–3 after ICH, and improved short-term neurological function outcome of mNSS scores and rotarod test on days 1–5 after ICH induction. Previous studies demonstrated that OPN contains a conserved arginine-glycine-aspartic acid (RGD) amino acid sequence initiating cell
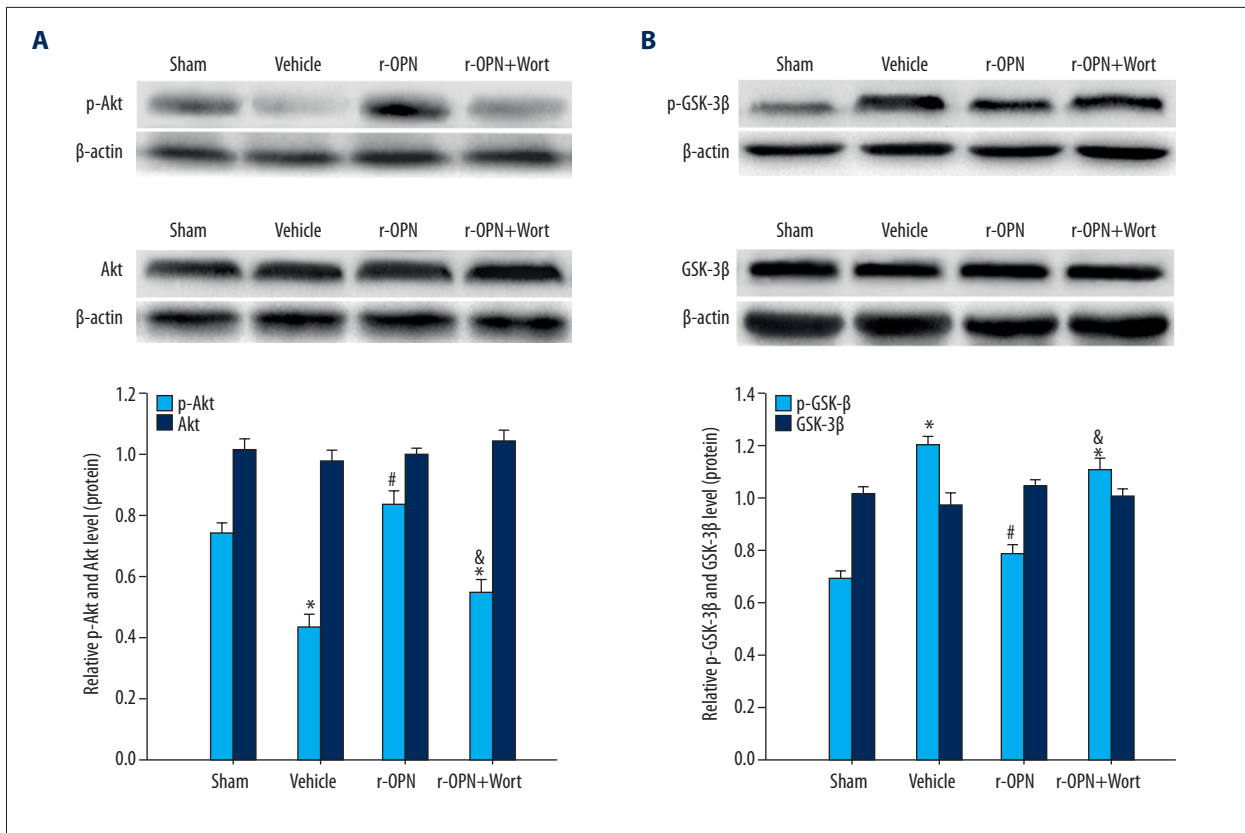
Figure 5. r-OPN affects p-Akt and p-GSK-3β protein expression 24 h after ICH or sham. Representative Western blots and densitometric quantification of p-Akt/β-actin and total Akt/β-actin (**A**). Representative Western blots and densitometric quantification of p-GSK-3β/β-actin and total GSK-3β/β-actin (**B**). Data are presented as the mean ±SEM (* $P<0.05$ compared with sham, # $P<0.05$ compared with vehicle, & $P<0.05$ compared with r-OPN, n=6–8/group).

signaling events upon integrin binding, and it promotes survival through the PI3K/Akt signaling pathway [35]. In addition, suppression of the apoptosis has been suggested to reduce brain edema and improve functional outcomes in experimentally induced ICH [36]. Therefore, we explored whether the neuroprotective mechanism of r-OPN was mediated by suppressing the cell apoptosis-related PI3K/Akt/GSK-3β signaling pathway. Animals receiving r-OPN treatment showed neuroprotective effects compared with vehicle group. When we administered PI3K inhibitor wortmannin and r-OPN, neurological impairment and brain edema were not alleviated compared with the r-OPN group. Our findings further confirm previous findings that wortmannin alone did not worsen the behavioral outcome and brain edema compared with the vehicle group after ICH [36]. These results indicate that r-OPN exerts neuroprotective effects through the PI3K/Akt signaling pathway.

At the molecular level, the Bcl-2 family proteins play important roles in intrinsic apoptotic pathway [37,38]. The family is divided into anti-apoptotic proteins such as Bcl-2 and pro-apoptotic proteins. Bax induces apoptosis, and Bax/Bcl-2 ratio is often used to represent the extent of apoptosis [39,40].

CC3 is an important marker of apoptosis [40]. In the present study, ICH induced an imbalance of Bax/Bcl-2 and increased the CC3 expression. r-OPN downregulated the ratio of Bax/Bcl-2 expression more toward the levels found in the sham group and also decreased the expression of CC3. We used TUNEL to detect apoptotic cell death and observed a significantly reduced density of TUNEL-positive cells in the r-OPN treatment group. r-OPN inhibited the apoptosis during the process of ICH, whereas r-OPN plus the wortmannin treatment upregulated the ratio of Bax/Bcl-2, increased the expression of CC3, and the number of TUNEL-positive cells increased significantly. Therefore, we explored whether the neuroprotection and the cell apoptosis suppression mechanism of r-OPN were mediated via the PI3K/Akt signal pathway.

Akt, a serine/threonine kinase, is a primary mediator of the downstream effects of phosphatidylinositol-3 kinase (PI3K), coordinating a variety of intracellular signals and controlling cell responses to extrinsic stimuli and regulating cell proliferation and survival [42]. The pro-apoptotic role of GSK-3β is an important downstream target of the Akt signaling pathway [43]. GSK-3β has been shown to participate in apoptosis in several

cell types and is known to be an upstream regulator of programmed cell death, which is particularly abundant in the CNS [44,45]. Dysregulation of GSK-3b activity is believed to play a key role in the pathogenesis of central nervous system chronic and acute disorders such as ischemic stroke, and traumatic brain injury [18,20]. Akt activation promotes cell survival by phosphorylation and subsequent inactivation of GSK-3β [21]. In the present study, r-OPN treatment significantly increased the expression of activated Akt (p-Akt, Ser473) at 24 h after ICH, which thereby successively reduced the expression of activated GSK-3β (p-GSK-3β, Ser9). r-OPN treatment reduced cell apoptosis and expression of apoptosis-related proteins. When we used PI3K inhibitor wortmannin combined with r-OPN, the levels of activated Akt protein and activated GSK-3β protein were similar to levels in the vehicle group. The wortmannin plus r-OPN treatment did not reduce the incidence of cell apoptosis after ICH in rats. Our results support r-OPN-mediated neuroprotection in a rat model of ICH, primarily via activation of the PI3K/Akt, and inhibited GSK-3β. However, certain physiological processes involving OPN partly depend on its cleavage by thrombin [10]. Thrombin-cleaved OPN fragments are strongly chemotactic for the endothelial cells, and help promote new blood vessel formation *in vitro* [10]. Thrombin is produced in the brain immediately after ICH [46]. Whether r-OPN following thrombin cleavage has positive effects on neuroprotection after ICH *in vivo* should be further explored.

Conclusions

In summary, our study demonstrated that r-OPN protected against ICH injury and improved neurological function by reducing apoptosis *in vivo*. Moreover, r-OPN exerted its anti-apoptotic effect through the PI3K/Akt/GSK-3β signaling pathway. In conclusion, the elucidation of the neuroprotective action of r-OPN in the current study adds to a growing literature suggesting the potential beneficial role for this factor in ICH.

Conflicts of interest

None.

References:

1. Steiner T, Alshahi SR, Beer R et al: European Stroke Organisation (ESO) guidelines for the management of spontaneous intracerebral hemorrhage. Int J Stroke, 2014; 9(7): 840–55

2. Lee SH, Park KJ, Park DH et al: Factors associated with clinical outcomes in patients with primary intraventricular hemorrhage. Med Sci Monit, 2018; 24: 1401–12

3. Lu Q, Chen L, Zeng J et al: Clinical features of liver cancer with cerebral hemorrhage. Med Sci Monit, 2016; 22: 1716–23

4. Broderick JP, Adams HP, Barsan W et al: Guidelines for the management of spontaneous intracerebral hemorrhage. Stroke, 1999; 30(5): 905–15

5. Xi G, Keep R F, Hoff J T: Mechanisms of brain injury after intracerebral haemorrhage. Lancet Neurol, 2006; 5(1): 53–63

6. Gong C, Boulis N, Qian J et al: Intracerebral hemorrhage-induced neuronal death. Neurosurgery, 2001; 48(4): 875–83

7. Matsushita K, Meng W, Wang X et al: Evidence for apoptosis after intracerebral hemorrhage in rat striatum. J Cerebr Blood F Met, 2000; 20: 396–404

8. Qureshi AI, Suri MF, Ostrow PT et al: Apoptosis as a form of cell death in intracerebral hemorrhage. Neurosurgery, 2003; 52(5): 1041-7; discussion 1047–48

9. Yang D, Han Y, Zhang J et al: Improvement in recovery after experimental intracerebral hemorrhage using a selective cathepsin B and L inhibitor: Laboratory investigation. J Neurosurg, 2011; 114(4): 1110–16

10. Denhardt DT, Noda M, O'Regan AW et al: Osteopontin as a means to cope with environmental insults: regulation of inflammation, tissue remodeling, and cell survival. J Clin Invest, 2001; 107(9): 1055–61

11. Maetzler W, Berg D, Schalamberidze N et al: Osteopontin is elevated in Parkinson's disease and its absence leads to reduced neurodegeneration in the MPTP model. Neurobiol Dis, 2007; 25(3): 473–82

12. Matusan-Ilijas K, Behrem S, Jonjic N et al: Osteopontin expression correlates with angiogenesis and survival in malignant astrocytoma. Pathol Oncol Res, 2008; 14(3): 293–98

13. Meller R, Stevens SL, Minami M et al: Neuroprotection by osteopontin in stroke. J Cerebr Blood F Met, 2005; 25(2): 217–25

14. Wu B, Ma Q, Suzuki H et al: Recombinant osteopontin attenuates brain injury after intracerebral hemorrhage in mice. Neurocrit Care, 2011; 14(1): 109–17

15. He J, Liu M, Liu Z et al: Recombinant osteopontin attenuates experimental cerebral vasospasm following subarachnoid hemorrhage in rats through an anti-apoptotic mechanism: Brain Res, 2015; 1611: 74–83

16. Cohen P, Frame S: The renaissance of GSK3. Nat Rev Mol Cell Biol, 2001; 2(10): 769–76

17. Ougolkov AV, Fernandez-Zapico ME, Savoy DN et al: Glycogen synthase kinase-3β participates in nuclear factor κB-mediated gene transcription and cell survival in pancreatic cancer cells. Cancer Res, 2005; 65(6): 2076–81

18. Valerio A, Bertolotti P, Delbarba A et al: Glycogen synthase kinase-3 inhibition reduces ischemic cerebral damage, restores impaired mitochondrial biogenesis and prevents ROS production. J Neurochem, 2011; 116(6): 1148–59

19. Krafft P R, Altay O, Rolland WB et al: α7 nicotinic acetylcholine receptor agonism confers neuroprotection through GSK-3β inhibition in a mouse model of intracerebral hemorrhage. Stroke, 2012; 43(3): 844–50

20. Shapira M, Licht A, Milman A et al: Role of glycogen synthase kinase-3β in early depressive behavior induced by mild traumatic brain injury. Mol Cell Neurosci, 2007; 34(4): 571–77

21. Jope RS, Johnson GVW: The glamour and gloom of glycogen synthase kinase-3. Trends Biochem Sci, 2004; 29(2): 95–102

22. Chen L, Xiang Y, Kong L et al: Hydroxysafflor yellow a protects against cerebral ischemia–reperfusion injury by anti-apoptotic effect through PI3K/Akt/GSK3β pathway in rat. Neurochem Res, 2013; 38(11): 2268–75

23. Yang JT, Lee TH, Lee IN et al: Dexamethasone inhibits ICAM-1 and MMP-9 expression and reduces brain edema in intracerebral hemorrhagic rats. Acta Neurochir, 2011; 153(11): 2197–203

24. Laskowitz DT, Lei B, Dawson HN et al: The apoE-mimetic peptide, COG1410, improves functional recovery in a murine model of intracerebral hemorrhage. Neurocrit Care, 2012; 16(2): 316–26

25. Toyoshima A, Yasuhara T, Kameda M et al: Intra-arterial transplantation of allogeneic mesenchymal stem cells mounts neuroprotective effects in a transient ischemic stroke model in rats: Analyses of therapeutic time window and its mechanisms. Plos One, 2015; 10(6): e0127302

26. Hamm RJ, Pike BR, O'Dell DM et al: The rotarod test: an evaluation of its effectiveness in assessing motor deficits following traumatic brain injury. J Neurotraum, 1994; 11(2): 187–96

27. Zhang S, Qi Y, Xu Y et al. Protective effect of flavonoid-rich extract from *Rosa laevigata Michx* on cerebral ischemia-reperfusion injury through suppression of apoptosis and inflammation. Neurochem Int, 2013; 63(5): 522–32

28. Spencer RL, Kalman BA, Cotter CS et al: Discrimination between changes in glucocorticoid receptor expression and activation in rat brain using western blot analysis. Brain Res, 2000; 868(2): 275–86

29. Belur PK, Chang JJ, He S et al: Emerging experimental therapies for intracerebral hemorrhage: targeting mechanisms of secondary brain injury. Neurosurg Focus, 2013; 34(5): E9

30. Geske FJ, Lieberman R, Strange R et al: Early stages of p53-induced apoptosis are reversible. Cell Death Differ, 2001; 8(2): 182–91

31. Rangaswami H, Bulbule A, Kundu GC: Osteopontin: Role in cell signaling and cancer progression. Trends Cell Biol, 2006; 16(2): 79–87

32. Schroeter M, Zickler P, Denhardt DT et al: Increased thalamic neurodegeneration following ischaemic cortical stroke in osteopontin-deficient mice. Brain, 2006; 129(6): 1426–37

33. Xie Y, Sakatsume M, Nishi S et al: Expression, roles, receptors, and regulation of osteopontin in the kidney. Kidney Int, 2001; 60(5): 1645–57

34. Chidlow G, Wood JPM, Manavis J et al: Expression of osteopontin in the rat retina: Effects of excitotoxic and ischemic injuries. Invest Ophth Vis Sci, 2008; 49(2): 762–71

35. Robertson BW, Chellaiah MA: Osteopontin induces β-catenin signaling through activation of Akt in prostate cancer cells. Exp Cell Res, 2010; 316(1): 1–11

36. Wang T, Huang Y, Zhang M et al: [Gly14]-Humanin offers neuroprotection through glycogen synthase kinase-3β inhibition in a mouse model of intracerebral hemorrhage. Behav Brain Res, 2013; 247: 132–39

37. Ola MS, Nawaz M, Ahsan H: Role of Bcl-2 family proteins and caspases in the regulation of apoptosis. Mol Cell Biochem, 2011; 351(1–2): 41–58

38. Zhu H, Gui Q, Hui X et al. TGF-β1/Smad3 signaling pathway suppresses cell apoptosis in cerebral ischemic stroke rats. Med Sci Monit, 2018; 24: 366–76

39. Gross A, McDonnell JM, Korsmeyer SJ: BCL-2 family members and the mitochondria in apoptosis. Gene Dev, 1999; 13(15): 1899–911

40. Raisova M, Hossini AM, Eberle J et al: The Bax/Bcl-2 ratio determines the susceptibility of human melanoma cells to CD95/Fas-mediated apoptosis. J Invest Dermatol, 2001; 117(2): 333–40

41. Garwood ER, Kumar AS, Baehner FL et al: Fluvastatin reduces proliferation and increases apoptosis in women with high grade breast cancer. Breast Cancer Res Treat, 2010; 119(1): 137–44

42. Chang F, Lee JT, Navolanic PM et al: Involvement of PI3K/Akt pathway in cell cycle progression, apoptosis, and neoplastic transformation: A target for cancer chemotherapy. Leukemia, 2003; 17(3): 590–603

43. Reis CR, Chen PH, Srinivasan S et al: Crosstalk between Akt/GSK3β signaling and dynamin-1 regulates clathrin-mediated endocytosis. Embo J, 2015; 34(16): 2132–46

44. Chen L, Wei X, Hou Y et al: Tetramethylpyrazine analogue CXC195 protects against cerebral ischemia/reperfusion-induced apoptosis through PI3K/Akt/GSK3β pathway in rats. Neurochem Int, 2014; 66: 27–32

45. Jiang L, Xia Q, Dong X et al: Neuroprotective effect of breviscapine on traumatic brain injury in rats associated with the inhibition of GSK3β signaling pathway. Brain Res, 2017; 1660: 1–9

46. Hua Y, Keep RF, Gu Y et al: Thrombin and brain recovery after intracerebral hemorrhage. Stroke, 2009; 40(3 Suppl. 1): S88–89